https://doi.org/10.5194/hess-2020-535
Preprint. Discussion started: 16 November 2020

Hydrology and Earth System Sciences
Discussions

Attribution of growing season evapotranspiration variability considering snowmelt and vegetation changes in the arid alpine basins

Tingting Ning[ab]*, Zhi Li[c], Qi Feng[ab] , Zongxing Li[ab] and Yanyan Qin[ab]

[a]*Key Laboratory of Ecohydrology of Inland River Basin, Northwest Institute of Eco-Environment and Resources, Chinese Academy of Sciences, Lanzhou, 730000, China*

[b]*Qilian Mountains Eco-environment Research Center in Gansu Province, Lanzhou, 730000, China*

[c]*College of Natural Resources and Environment, Northwest A&F University, Yangling, Shaanxi, 712100, China*

* Correspondence to: Tingting Ning (ningting2012@126.com)

https://doi.org/10.5194/hess-2020-535
Preprint. Discussion started: 16 November 2020

Abstract: Previous studies have successfully applied variance decomposition frameworks based on the Budyko equations to determine the relative contribution of variability in precipitation, potential evapotranspiration (E_0), and total water storage changes (ΔS) to evapotranspiration variance (σ_{ET}^2) on different time-scales; however, the effects of snowmelt (Q_m) and vegetation (M) changes have not been incorporated into this framework in snow-dependent basins. Taking the arid alpine basins in the Qilian Mountains in northwest China as the study area, we extended the Budyko framework to decompose the growing season σ_{ET}^2 into the temporal variance and covariance of rainfall (R), E_0, ΔS, Q_m, and M. The results indicate that the incorporation of Q_m could improve the performance of the Budyko framework on a monthly scale; σ_{ET}^2 was primarily controlled by the R variance with a mean contribution of 63%, followed by the coupled R and M (24.3%) and then the coupled R and E_0 (14.1%). The effects of M variance or Q_m variance cannot be ignored because they contribute to 4.3% and 1.8% of σ_{ET}^2, respectively. By contrast, the interaction of some coupled factors adversely affected σ_{ET}^2, and the 'out-of-phase' seasonality between R and Q_m had the largest effect (−7.6%). Our methodology and these findings are helpful for quantitatively assessing and understanding hydrological responses to climate and vegetation changes in snow-dependent regions on a finer time-scale.

Keywords: evapotranspiration variability; snowmelt; vegetation; attribution

1 Introduction

Actual evapotranspiration (*ET*) drives energy and water exchanges among the hydrosphere, atmosphere, and biosphere (Wang et al., 2007). The temporal variability in *ET* is, thus, the combined effect of multiple factors interacting across the soil–vegetation–atmosphere interface (Katul et al., 2012; Xu and Singh, 2005). Investigating the mechanism behind *ET* variability is also fundamental for understanding hydrological processes. The basin-scale *ET* variability has been widely investigated with the Budyko framework (Budyko, 1961, 1974); however, most studies are conducted on long-term or inter-annual scales and cannot interpret the short-term *ET* variability (e.g. monthly scales).

Short-term *ET* and runoff (Q_r) variance have been investigated recently for their dominant driving factors (Feng et al., 2020; Liu et al., 2019; Wu et al., 2017; Ye et al., 2015; Zeng and Cai, 2015; Zeng and Cai, 2016; Zhang et al., 2016a); to this end, an overall framework was presented by Zeng and Cai (2015) and Liu et al. (2019). Zeng and Cai (2015) decomposed the intra-annual *ET* variance into the variance/covariance of precipitation (P), potential evapotranspiration (E_0), and water storage change (ΔS) under the Budyko framework based on the work of Koster and Suarez (1999). Subsequently, Liu et al. (2019) proposed a new framework to identify the driving factors of global Q_r variance by considering the temporal variance of P, E_0, ΔS, and other factors such as the climate seasonality, land cover, and human impact. Although

https://doi.org/10.5194/hess-2020-535
Preprint. Discussion started: 16 November 2020

the proposed framework performs well for the *ET* variance decomposition, further research is necessary for considering additional driving factors and for studying regions with unique hydrological processes.

The impact of vegetation change should first be fully considered when studying the variability of *ET*. Vegetation change significantly affects the hydrological cycle through rainfall interception, evapotranspiration, and infiltration (Rodriguez-Iturbe, 2000; Zhang et al., 2016b). Higher vegetation coverage increases *ET* but reduces the ratio of Q_r to P (Feng et al., 2016). However, most of the existing studies on *ET* variance decomposition either ignored the effects of vegetation change or did not quantify its contributions. Vegetation change is closely related to the Budyko controlling parameters, and several empirical relationships have been successfully developed on long-term and inter-annual scales (Li et al., 2013; Liu et al., 2018; Ning et al., 2020; Xu et al., 2013; Yang et al., 2009). However, the relationship between vegetation and its controlling parameters on a finer time-scale has received less attention. As such, it is important to quantitatively investigate the contribution of vegetation change to *ET* variability on a finer time-scale.

Second, for snow-dependent regions, the water balance equation should be modified to consider the influence of snowmelt in short-term time scale, which has been the foundation for decomposing *ET* or runoff variance and is expressed as:

$$P = ET + Q_r + \Delta S, \tag{1}$$

where P, including liquid (rainfall) and solid (snowfall) precipitation, is the total water source of the hydrological cycle. However, this equation is unsuitable for regions where the land-surface hydrology is highly dependent on the winter mountain snowpack and spring snowmelt runoff. The global annual Q_r originating from snowmelt accounts for 20–70% of the total runoff, including west United States (Huning and AghaKouchak, 2018), coastal areas of Europe (Barnett et al., 2005), west China (Li et al., 2019b), northwest India (Maurya et al., 2018), south of the Hindu Kush (Ragettli et al., 2015), and high-mountain Asia (Qin et al., 2020). In these regions, the mountain snowpack serves as a natural reservoir that stores cold-season P to meet the warm-season water demand (Qin et al., 2020; Stewart, 2009). As such, the water balance equation in these regions on a short time-scale should be rewritten as:

$$R + Q_s = ET + Q_r + \Delta S, \tag{2}$$

where R is the rainfall, and Q_s is the snowmelt runoff. Many observations and modelling experiments have found that due to global warming, increasing temperatures would induce earlier runoff in the spring or winter and reduce the flows in summer and autumn (Barnett et al., 2005; Godsey et al., 2014; Stewart et al., 2005; Zhang et al., 2015). Therefore, the role of snowmelt change on ET variability in snow-dependent basins on a finer time-scale should be studied.

The overall objective of this study was to decompose the *ET* variance into the temporal variability of multiple factors considering vegetation and snowmelt change. The six cold alpine basins in the Qilian Mountains of northwest China were taken as an example study area. Specifically, we aimed to: (i) determine the dominant driving factor controlling the *ET* variance; (2) investigate the roles of vegetation and snowmelt change in the variance; and (3) understand the interactions among the controlling factors in *ET* variance. The proposed method will help quantify the hydrological response to changes in snowmelt and vegetation in snowmelt-dependent regions, and our results will prove to be insightful for water resource management in other similar regions worldwide.

2 Materials

2.1 Study area

Six sub-basins located in the upper reaches of the Heihe, Shiyang, and Shule rivers in the Qilian Mountains were chosen as the study area (Figure 1). They are important inland rivers in the dry region of northwest China. The runoff generated from the upper reaches contributes to nearly 70% of the water resources of the entire basin and thus plays an important role in supporting agriculture, industry development, and ecosystem maintenance in the middle and downstream rivers (Cong et al., 2017; Wang et al., 2010a). Snowmelt and in-mountain-generated rainfall make up the water supply system for the upper basins (Matin and Bourque, 2015), and the annual average *P* exceeds 450 mm in this region. At higher altitudes, as much as 600–700 mm of P can be observed (Yang et al., 2017). Nearly 70% of the total rainfall concentrates between June and September, while only 19% of the total rainfall occurs from March to June. Snowmelt runoff is an important water source (Li et al., 2012; Li et al., 2018; Li et al., 2016); in the spring, 70% of the runoff is supplied by snowmelt water (Wang and Li, 2001). Characterised by a continental alpine semi-humid climate, alpine desert glaciers, alpine meadows, forests, and upland meadows are the predominant vegetation distribution patterns (Deng et al., 2013). Furthermore, this region has experienced substantial vegetation changes and resultant hydrological changes in recent decades (Bourque and Mir, 2012; Du et al., 2019; Ma et al., 2008).

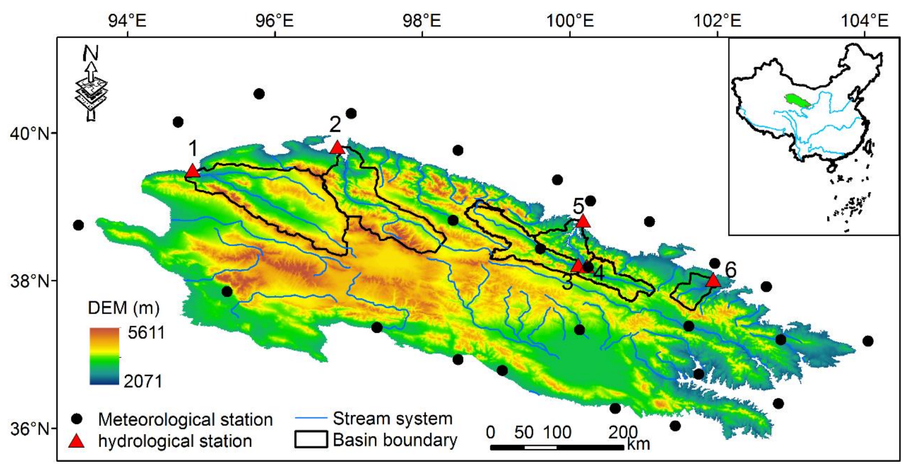

Figure 1 The six basins in China's northern Qilian Mountains. The Digital elevation data, at 30 m resolution, was provided by the Geospatial Data Cloud site, Computer Network Information Center, Chinese Academy of Sciences.

https://doi.org/10.5194/hess-2020-535
Preprint. Discussion started: 16 November 2020

2.2 Data

Daily climate data were collected for 25 stations distributed in and around the Qilian Mountains from the China Meteorological Administration. They comprised rainfall, air temperature, sunshine hours, and relative humidity and would be used to calculate the monthly E_0 using the Priestley and Taylor (1972) equation.

The monthly runoff at the Dangchengwan, Changmabu, Zhamashike, Qilian, Yingluoxia, and Shagousi hydrological stations were obtained for 2001–2014 from the Bureau of Hydrology and Water Resources, Gansu Province. The sum of the monthly soil moisture and plant canopy surface water with a resolution of $0.25^{\circ} \times 0.25^{\circ}$ from the Global Land Data Assimilation System (GLDAS) Noah model was used to estimate the total water storage. The monthly ΔS was calculated as the water storage difference between two neighbouring months. Eight-day composites of the MODIS MOD10A2 Version 6 snow cover product from the MODIS TERRA satellite were used to produce the monthly snow cover area (*SCA*) of each basin. The *SCA* data were used to drive the snowmelt runoff model.

A monthly normalised difference vegetation index (*NDVI*) at a spatial resolution of 1 km from the MODIS MOD13A3.006 product was used to assess the vegetation coverage (*M*), which can be calculated from the method described in Yang et al. (2009). A land-use map with 1-km resolution in 2010 was used to determine the forest area of each basin, and it was provided by the Data Centre for Resources and Environmental Sciences of the Chinese Academy of Sciences. The percentages of forestland area to the whole basin area served as the F for each basin (%).

3 Methods

3.1 The Budyko framework at monthly scales

Probing the ET variability in the growing season can provide basic scientific reference points for agricultural activities and water resource planning and management (Li et al., 2015; Wagle and Kakani, 2014). Thus, we focus on the growing season ET variability on a monthly scale in this study.

Among the mathematical forms of the Budyko framework, this study employed the function proposed by Choudhury (1999) and Yang et al. (2008) to assess the basin water balance for good performance (Zhou et al., 2015):

$$ET = \frac{P \times E_0}{(P^n + E_0^n)^{1/n}}, \tag{3}$$

where n is the controlling parameter of the Choudhury–Yang equation, and P is the total available water supply for ET. In Equation 2, however, the available water supply (P_e) includes the rainfall, snowmelt runoff, and water storage change in the snow-dependent basins on a finer time-scale, which can be rewritten as:

https://doi.org/10.5194/hess-2020-535
Preprint. Discussion started: 16 November 2020

$$P_e = R + Q_S - \Delta S. \quad (4)$$

Equation 3 can thus be redefined as follows:

$$ET_i = \frac{(R_i + Q_{s_i} - \Delta S_i) \times E_{0_i}}{((R_i + Q_{s_i} - \Delta S_i)^{n_i} + E_{0_i}^{n_i})^{1/n_i}}, \quad (5)$$

where i indicates each month of the growing season (April to September). After estimating the monthly ET of the growing season using Equation 2, the values of n for each month can be obtained via Equation 5.

3.2 Estimating the equivalent of snowmelt runoff

With the developed relationship between snowmelt and air temperature (Hock, 2003), the degree-day model simplifies the complex processes and performs well, so it is widely used in snowmelt estimation (Griessinger et al., 2016; Rice et al., 2011; Semadeni-Davies, 1997; Wang et al., 2010a). This study estimated the monthly Q_s using the degree-day model following the Wang et al. (2015) procedure. Specifically, the water equivalent of snowmelt (W, mm) during the period m can be calculated as:

$$\sum_{i=1}^{m} W_i = DDF \sum_{i=1}^{m} T_i^{+}, \quad (6)$$

where DDF denotes the degree-day factor (mm/day · °C), and T^{+} is the sum of the positive air temperatures of each month. After obtaining W, the monthly Q_s of each elevation zone can be expressed as:

$$\sum_{i=1}^{m} Q_{Si} = \sum_{i=1}^{m} W_i \, SCA_i, \tag{7}$$

where SCA_i is the snow cover area of each elevation zone.

According to Gao et al. (2011), the *DDF* values of Basins 1–6 were set to 3.4, 3.4, 4.0, 4.0, 4.0, and 1.7 mm/day · °C, respectively. The six basins were divided into seven elevation zones with elevation differences of 500 m. The sum of Q_s in each elevation zone could be considered as the total Q_s of each basin. Previous studies have found that the major snow melting period is from March to July in this area (Wang and Li, 2005; Wu et al., 2015); furthermore, the MODIS snow product also showed that the *SCA* decreased significantly at the end of July. Thus, the snowmelt runoff from April to July for the growing season was estimated in this study.

3.3 Relationship between the Budyko controlling parameter and vegetation change

The relationships between the monthly parameters n and M for each basin in the growing season for 2001–2014 are presented in Figure 2. It can be seen that parameter n was significantly positively related to M in all six basins ($p < 0.05$), which means that ET increased with increasing vegetation conditions under the given climate conditions.

In Equation 5, when $n \to 0$, $ET \to 0$, which means M should have the following limiting conditions: if $ET \to 0$, $T \to 0$ (transpiration), and thus $M \to 0$. Considering the relationship

https://doi.org/10.5194/hess-2020-535
Preprint. Discussion started: 16 November 2020

shown in Figure 2 and the above limiting conditions, the general form of parameter n can be expressed as follows:

$$n = a \times M^{b}, \tag{8}$$

where a and b are constants, and their specific values for each basin are fitted in Figure 2.

https://doi.org/10.5194/hess-2020-535
Preprint. Discussion started: 16 November 2020

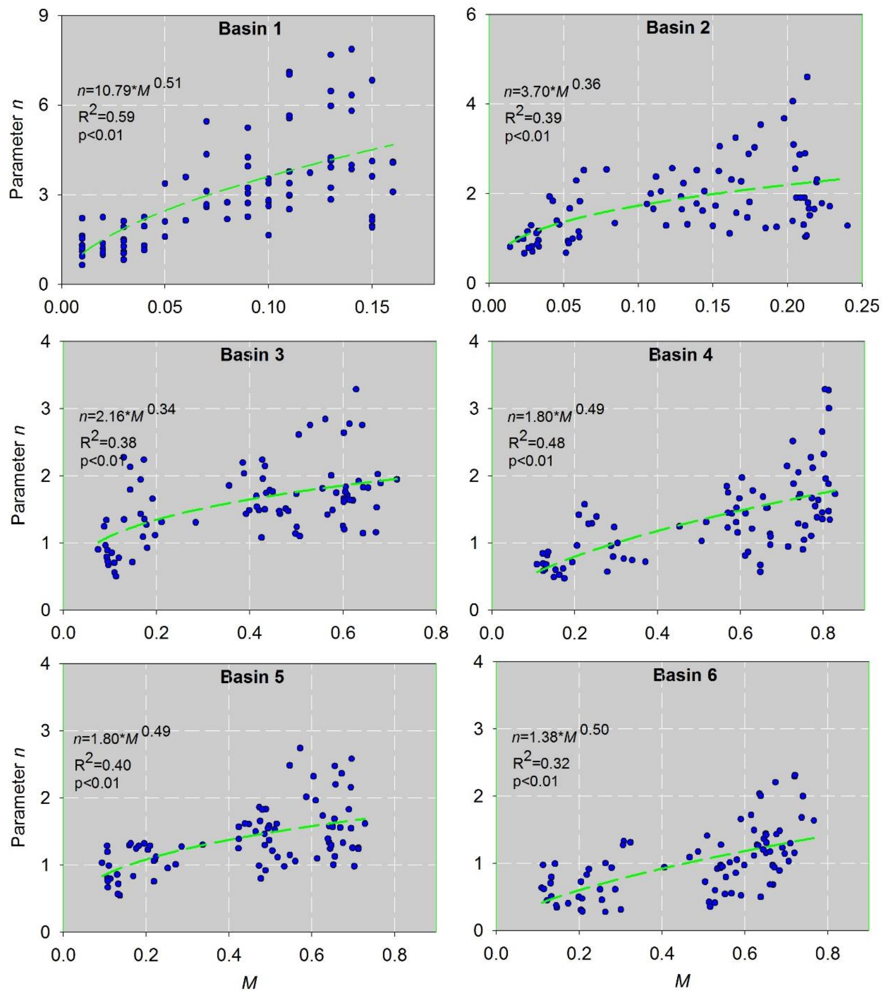

Figure 2 Relationships between the parameter *n* and the vegetation coverage for each basin on a monthly scale.

3.4 *ET* variance decomposition

Liu et al. (2019) proposed a framework to identify the driving factors behind the temporal variance of Q_r by combining the unbiased sample variance of Q_r with the total differentiation of Q_r changes. Here, we extended this method by considering the effects of changes in snowmelt runoff and vegetation coverage on ET variance.

By combining Equation 5 with Equation 8, Equation 5 can be simplified as $ET \approx f(R_i, Q_{si}, \Delta S_i, E_{0i}, M_i)$. Thus, the total differentiation of ET changes can be expressed as:

$$dET_i = \frac{\partial f}{\partial R} dR_i + \frac{\partial f}{\partial Q_s} dQ_{s_i} + \frac{\partial f}{\partial \Delta S} d\Delta S_i + \frac{\partial f}{\partial E_0} dE_{0_i} + \frac{\partial f}{\partial M} dM_i + \tau, \qquad (9)$$

where τ is the error. The partial differential coefficients can be calculated as:

$$\frac{\partial ET}{\partial R} = \frac{\partial ET}{\partial Q_s} = -\frac{\partial ET}{\partial \Delta S} = \frac{ET}{P_e} \times \left(\frac{E_0^n}{P_e^n + E_0^n}\right), \qquad (10a)$$

$$\frac{\partial ET}{\partial E_0} = \frac{ET}{E_0} \times \left(\frac{P_e^n}{P_e^n + E_0^n}\right), \qquad (10b)$$

$$\frac{\partial ET}{\partial M} = \frac{ET}{n} \left(\frac{\ln(P_e^n + E_0^n)}{n} - \frac{P_e^n lnP + E_0^n lnE_0}{P_e^n + E_0^n}\right) \times a \times b \times M^{b-1}. \qquad (10c)$$

The first-order approximation of ET changes in Equation 9 can be expressed as:

$$\Delta ET_i \approx \varepsilon_1 \Delta R_i + \varepsilon_2 \Delta Q_{s_i} + \varepsilon_3 \Delta S_i + \varepsilon_4 \Delta E_{0_i} + \varepsilon_5 \Delta M_i, \qquad (11)$$

where $\varepsilon_1 = \frac{\partial ET}{\partial R}$; $\varepsilon_2 = \frac{\partial ET}{\partial Q_s}$; $\varepsilon_3 = \frac{\partial ET}{\partial \Delta S}$; $\varepsilon_4 = \frac{\partial ET}{\partial E_0}$; $\varepsilon_5 = \frac{\partial ET}{\partial M}$.

The unbiased sample variance of ET is defined as:

$$\sigma_{ET}^2 = \frac{1}{N-1} \sum_{i=1}^{N} (ET_i - \overline{ET})^2 = \frac{1}{N-1} (\Delta ET_i)^2. \qquad (12)$$

Combining Equation 11 with Equation 12, σ_{ET}^2 can be decomposed as the contribution

https://doi.org/10.5194/hess-2020-535
Preprint. Discussion started: 16 November 2020

from different variance/covariance sources:

$$\sigma_{ET}^2 = \sum_{i=1}^{N}(\varepsilon_1 \Delta R_i + \varepsilon_2 \Delta Q_{s_i} + \varepsilon_3 \Delta S_i + \varepsilon_4 \Delta E_{0_i} + \varepsilon_5 \Delta M_i)^2. \tag{13}$$

Expanding Equation 13, σ_{ET}^2 can be further rewritten as:

$$\sigma_{ET}^2 = \varepsilon_1^2 \sigma_R^2 + \varepsilon_2^2 \sigma_{Q_s}^2 + \varepsilon_3^2 \sigma_{\Delta S}^2 + \varepsilon_4^2 \sigma_{E_0}^2 + \varepsilon_5^2 \sigma_M^2 + 2\varepsilon_1\varepsilon_2 \mathrm{cov}(R, Q_s) + 2\varepsilon_1\varepsilon_3 \mathrm{cov}(R, \Delta S) + 2\varepsilon_1\varepsilon_4 \mathrm{cov}(R, E_0) + 2\varepsilon_1\varepsilon_5 \mathrm{cov}(R, M) + 2\varepsilon_2\varepsilon_3 \mathrm{cov}(Q_s, \Delta S) + 2\varepsilon_2\varepsilon_4 \mathrm{cov}(Q_s, E_0) + 2\varepsilon_2\varepsilon_5 \mathrm{cov}(Q_s, M) + 2\varepsilon_3\varepsilon_4 \mathrm{cov}(E_0, \Delta S) + 2\varepsilon_3\varepsilon_5 \mathrm{cov}(M, \Delta S) + 2\varepsilon_4\varepsilon_5 \mathrm{cov}(E_0, M), \tag{14}$$

where σ represents the standard deviation, and *cov* represents the covariance. Equation 14 can be further simplified as:

$$\sigma_{ET}^2 = F(R) + F(Q_s) + F(\Delta S) + F(E_0) + F(M) + F(R\_Q_s) + F(R\_\Delta S) + F(R\_E_0) + F(R\_M) + F(Q_s\_\Delta S) + F(Q_s\_E_0) + F(Q_s\_M) + F(\Delta S\_E_0) + F(\Delta S\_M) + F(E_0\_M), \tag{15}$$

By separating out Equation 15, the contribution of each factor to σ_{ET}^2 can be calculated as:

$$C(X_{\mathrm{j}}) = \frac{F(X_j)}{\sigma_{ET}^2} \times 100\%, \tag{16}$$

where $C(X_{\mathrm{j}})$ is the contribution of factor $F(j)$ to σ_{ET}^2, and j = 1–15, representing the 15 factors in Equation 15.

https://doi.org/10.5194/hess-2020-535
Preprint. Discussion started: 16 November 2020

Hydrology and Earth System Sciences Discussions

4 Results and Discussion

4.1 Performance of the monthly Budyko framework

The importance of considering ΔS in the Budyko framework on a finer time-scale has been underscored by several studies (Chen et al., 2013; Du et al., 2016; Liu et al., 2019; Zeng and Cai, 2015); however, the effects of Q_m in snowmelt-dependent basins are mostly ignored. Here, the monthly Budyko curves—scaled by different available water supply values (P_e) for monthly series in the growing season—were compared. When $P_e = R$ and $P_e = R - \Delta S$, the data points of the monthly *ET* ratio and aridity index ($\phi = E_0/P_e$) in April and May were well below the Budyko curves in the six sub-basins; the monthly *ET* ratio was even negative during several years (Figure 3a,b), which means that local rain and water storage are not the only sources of *ET* in this area, especially in the spring. When $P_e = R + Q_m$, the outlier points in April and May were significantly improved (Figure 3c), suggesting that Q_m is an important source of spring *ET*. Similarly, Wang and Li (2001) also determined that 70% of the runoff is supplied by snowmelt water in the spring in this area. Compared to the points in Figures 3a–c, all the points focused on Budyko's curves more closely in each basin when $P_e = R + Q_m - \Delta S$ (Figure 3d). Therefore, considering Q_m and ΔS in the water balance equation can improve the performance of the Budyko framework in snowmelt-dependent basins on a monthly scale.

254 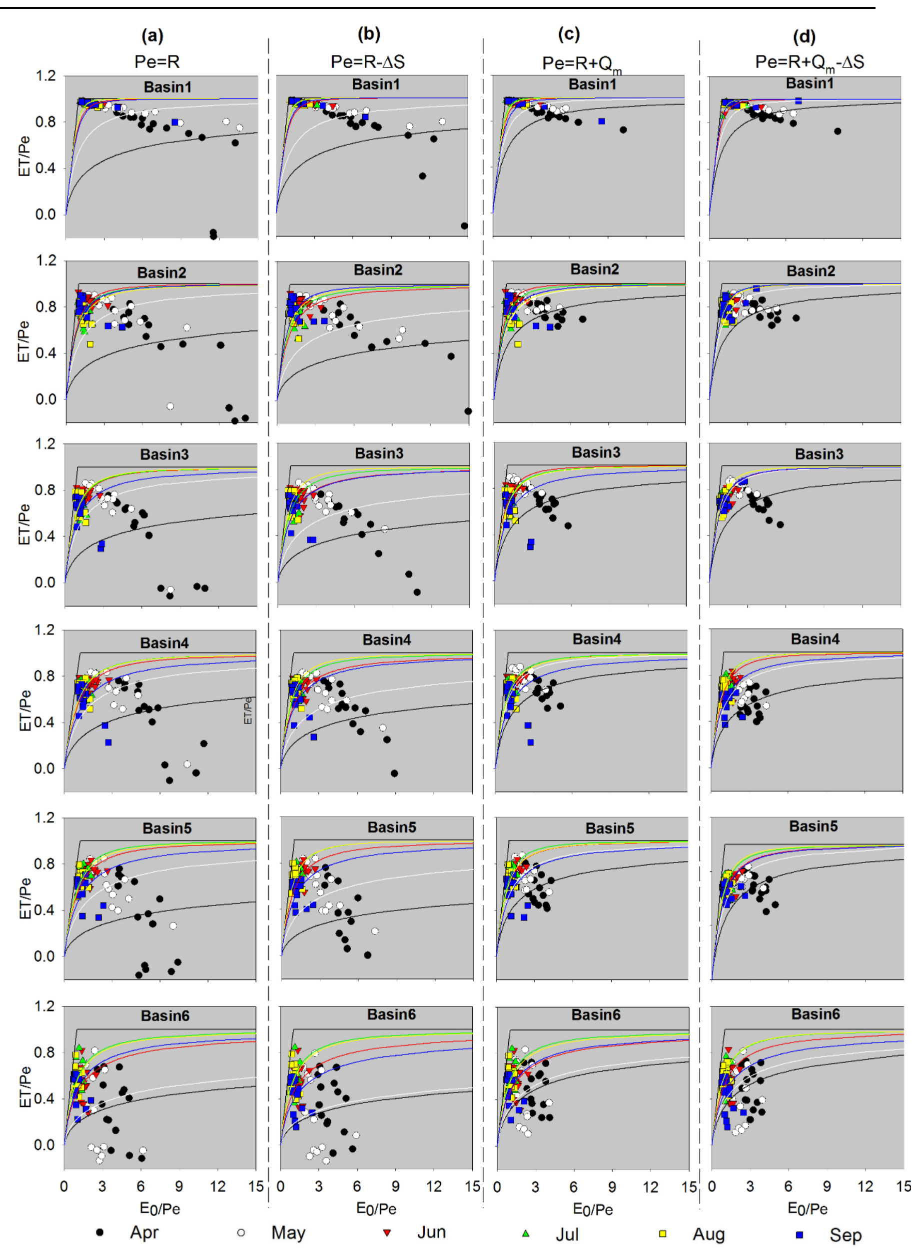

255 Figure 3 Plots for the aridity index vs. evapotranspiration index scaled by the available water

256 supply for monthly series in the growing season. The total water availability is (a) R, (b) $R - \Delta S$,

257 (c) $R + Q_m$, and (d) $R + Q_m - \Delta S$. The n value for each Budyko curve is fitted by long-term

https://doi.org/10.5194/hess-2020-535
Preprint. Discussion started: 16 November 2020

averaged monthly data.

4.2 Variations in the growing season water balance

The mean and standard deviation (σ) for each item in the growing season water balance in the six basins are summarised in Tables 1 and 2. The proportion of ΔS in the water balance was small, with a mean value of 1.2 mm; however, its intra-annual fluctuation was relatively large, with a $\sigma_{\Delta S}$ of 5.3 mm, and $\sigma_{\Delta S}$ was even as high as 9.0 mm in Basin 6. Compared to ΔS, Q_m represented a larger proportion of the water balance with a mean of 8.5±6.5 mm, indicating its important role in the basin water supply. For this region, the water supply of ET was not only R but also included Q_m and ΔS. Consequently, the mean monthly ET generally approached R (55.8±27.4 mm) or higher values in Basin 1.

Table 1 Averaged monthly hydrometeorological characteristics and vegetation coverage in the growing season (2001–2014).

ID	Station	Area	R	Q_m	ΔS	E_0	M	n	E
1	Dangchengwan	14325	57.2	8.6	0.7	126.7	0.08	3.08	59.1
2	Changmabu	10961	68.9	10.8	1.1	123.0	0.13	1.79	59.3
3	Zhamashike	4986	73.5	10.6	1.5	120.3	0.40	1.59	59.1
4	Qilian	2452	74.5	9.0	1.4	116.8	0.44	1.37	54.9
5	Yingluoxia	10009	77.2	7.4	1.1	117.4	0.53	1.35	55.1
6	Shagousi	1600	83.5	4.8	1.4	116.3	0.48	1.01	47.1

The change patterns of the monthly R, ΔS, Q_m, and ET during the growing season are presented in Figure 4 and Supplementary Figures S1–S3. R exhibited a regular

https://doi.org/10.5194/hess-2020-535
Preprint. Discussion started: 16 November 2020

unimodal trend, with a maximum value occurring in July. The maximum Q_m appeared in May, which is a result that is in agreement with previous studies in this region (Wang and Qin, 2017; Zhang et al., 2016c). The peak of ΔS lagged that of Q_m for one month in Basins 1–4 and three months in Basins 5–6, indicating a recharge of soil water by snowmelt. Yang et al. (2015) also detected the time differences between ΔS and Q_m and found that ΔS had a time lag of 3–4 months more than did Q_m in the Tarim River Basin, another arid alpine basin in north-western China with hydroclimatic conditions similar to those of the study region. Further, the abundant R in July should contribute to more available water for ΔS; however, the ΔS in July was relatively small. This can be partially explained by the higher water consumption, i.e. the ET in July. In a manner similar to the change pattern of R, ET exhibited a unimodal trend, suggesting the crucial role of R.

285 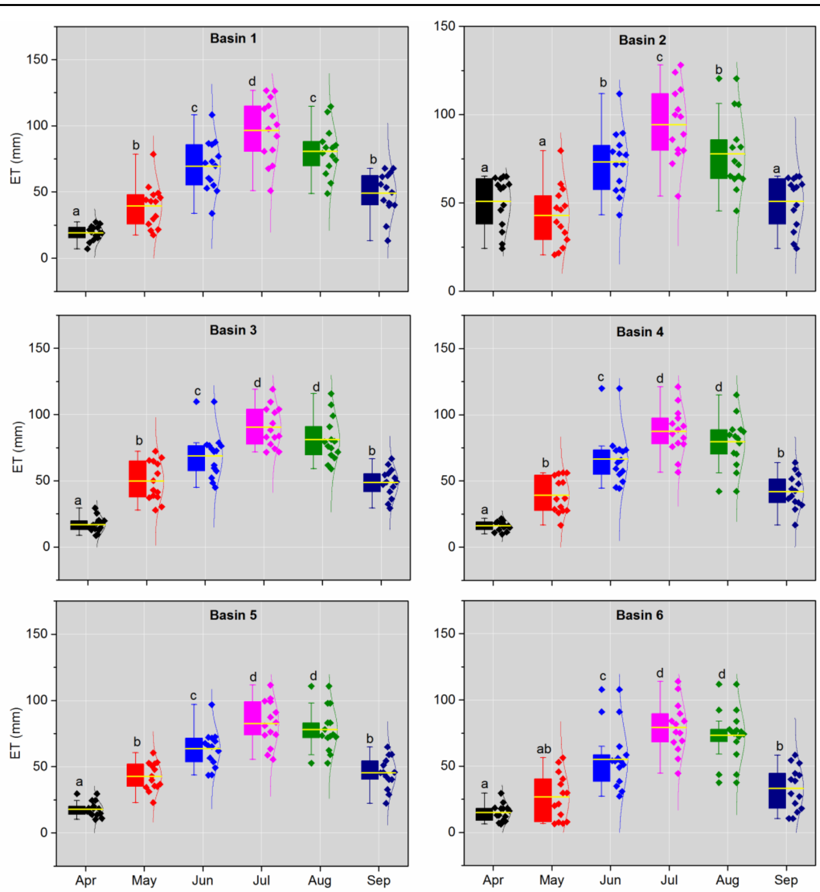

286 Figure 4 Variations in the monthly *ET* for each basin during 2001–2014. A distribution curve is

287 shown to the right side of each box plot, and the data points are represented by diamonds.

288 Different letters indicate significant differences at $p < 0.05$.

289 **4.3 Controlling factors of the *ET* variance**

290 The contributions of R, E_0, Q_m, ΔS, and M to σ_{ET}^2 for each basin are shown in Figure

291 5. The results showed that the variance of these five factors could explain σ_{ET}^2, with the

292 total contribution rates ranging from 56.5% (Basin 6) to 98.6% (Basin 1). With the

https://doi.org/10.5194/hess-2020-535
Preprint. Discussion started: 16 November 2020

decreasing ϕ from Basin 1 to Basin 6, C(R) showed an increasing trend, ranging from 40.6% to 94.2%; conversely, C(E_0) exhibited a decreasing trend, ranging from 0.2% to 4.1%. This result indicated that R played a key role in σ_{ET}^2 in this region. Similarly, Zhang et al. (2016a) found that C(P) increased rapidly with increasing ϕ, whereas C(E_0) decreased rapidly based on 282 basins in China. Our results are also consistent with previous conclusions that changes in ET or Q_r are dominated by changes in water conditions rather than by energy conditions in dry regions (Berghuijs et al., 2017; Yang et al., 2006; Zeng and Cai, 2016; Zhang et al., 2016a).

The M variance had the second largest contribution to σ_{ET}^2 with a mean C(M) value of 4.3% for the six basins. Specifically, C(M) showed an increasing trend from 0.5% to 9.5% with decreasing ϕ, implying that the contribution of the vegetation change to the ET variance was larger in the humid basin. This can be explained by the fact that better vegetation conditions, especially forest cover, could have a stronger impact on ET variance. With the estimated percentages of forestland relative to the whole basin (F) (Table S1), we found that the M variance indeed had a larger contribution to σ_{ET}^2 in Basins 4–6 with a higher F. Wei et al. (2018) showed that the global average variation in the annual Q_r due to the vegetation cover change was 30.7±22.5% in forest-dominated regions on long-term scales, which was higher than our results because of their higher forest cover.

The contribution of the Q_m variance ranked third with a mean value of 1.8%. Similar to

C(R), C(Q_m) showed a downward trend from Basin 1 to Basin 6, ranging from 2.9% to 0.4%. The larger C(Q_m) can be explained by the larger variance in Q_m in Basins 2–4 (σ values in Table 2). However, the Q_m in Basin 1 was only 8.6 mm, and C(Q_m) was the largest in all six sub-basins (2.9%). This is because the contribution of each variable to σ_{ET}^2 was not only the product of its variance value but also relied on the elasticity coefficient of σ_{ET}^2 according to Equation 13. The ε_{Q_m} value was the largest in Basin 1 and thus led to the largest C(Q_m). In addition, shifts in the snowmelt period can also partially explain the positive contribution of the Q_m variance. Like many snow-dominated regions of the world (Barnett et al., 2005), climate warming shifted the timing of snowmelt earlier in the spring in the Qilian Mountains (Li et al., 2012). Earlier snowmelt due to a warmer atmosphere resulted in increased soil moisture and a greater proportion of Q_m to ET (Barnhart et al., 2016; Bosson et al., 2012).

Previous studies have considered that most precipitation changes are transferred to water storage (Wang and Hejazi, 2011); thus, ΔS has distinct impacts on the intra-annual ET or Q_r variance in arid regions (Ye et al., 2015; Zeng and Cai, 2016; Zhang et al., 2016a). However, the study region under investigation has a small C(ΔS) with a mean value of 1.02%, which is likely to be caused by the vegetation conditions and time-scale. First, the six basins have good vegetation conditions compared to other arid basins; consequently, plant transpiration and rainfall interception consume most of the water supply and reduce the transformation of rainfall to water storage. This is

https://doi.org/10.5194/hess-2020-535
Preprint. Discussion started: 16 November 2020

consistent with previous studies that showed that the fractional contribution of transpiration to *ET* would increase with increasing woody cover (Villegas et al., 2010; Wang et al., 2010b). Second, the large contribution of ΔS to the intra-annual *ET* or Q_r variance in arid regions is mostly detected at monthly scales. The smaller ΔS in the non-growing season will increase the annual value of $\sigma_{\Delta S}$. However, this study focused on the growing season with a smaller $\sigma_{\Delta S}$, which consequently led to a lower C(ΔS).

4.4 Interaction effects between controlling factors on the *ET* variance

The interaction effect of two factors on the *ET* variance was represented by their covariance coefficients using Equations 14 and 15 (Figure 5). Among the ten groups of interaction effects, the coupled *R* and *M* had the largest contribution to the *ET* variance, with a mean value of 24.3%. The positive covariance of *R* and *M* indicated that *M* changes in-phase with *R* (i.e. *R* occurred in the growing season), thus increasing the *ET* variance. C(R_M) showed an increasing trend from 9.9% to 34.6% with decreasing ϕ. With different water conditions, the types and proportions of the main ecosystems varied across basins. In particular, *F* showed an increasing trend with decreasing ϕ, which partially explained the spatial variations in C(R_M). Previous studies concluded that the differences in physiological and phenological characteristics of ecosystem types are likely to modulate the response of the ecosystem *ET* to climate variability (Bruemmer et al., 2012; Falge et al., 2002; Li et al., 2019a). For example, Yuan et al. (2010) found that, at the beginning of the growing season, a significantly higher *ET* was observed in evergreen needleleaf forests; however, during the middle term of the growing season (June–August), the ET was largest in deciduous broadleaf forests in a typical Alaskan basin.

As an indicator of climate seasonality, the covariance of R and E_0 indicates matching conditions between the water and energy supplies, such as the phase difference between the storm season and warm season. A positive cov(R, E_0) suggests an in-phase R change with E_0 and consequently increases the ET variance. In this study, following C(R_M), the coupled R and E_0 had a large impact on the ET variance with a mean contribution of 14.1%. With a typical temperate continental climate, the study area has in-phase water and energy conditions; however, its ET is limited by the water supply in spite of the abundant energy supply (Yang et al., 2006). The vegetation receives the largest water supply in the growing season and can vary its biomass seasonally in order to adapt to the R seasonality (Potter et al., 2005; Ye et al., 2016). Consequently, the impact of climate variability on ET variance was mainly reflected by the R seasonality in the study area.

In comparison, the interacting effects between R and Q_m, M and Q_m, R and ΔS, and Q_m and E_0 contributed negatively to the ET variance. Among them, the effect of the coupled R and Q_m was largest with a C(R_Q_m) of −7.6%. This may suggest that Q_m changes were out-of-phase with R. Specifically, the major snow melting period was from March to May, when snowmelt water accounts for ~70% of the water supply; however, ~ 65%

https://doi.org/10.5194/hess-2020-535
Preprint. Discussion started: 16 November 2020

Hydrology and Earth System Sciences
Open Access
Discussions
EGU

of the annual R occurred in the summer (June–August) (Li et al., 2019a). Overall, Q_m sustains the ET in the spring, but R supports the ET in the summer.

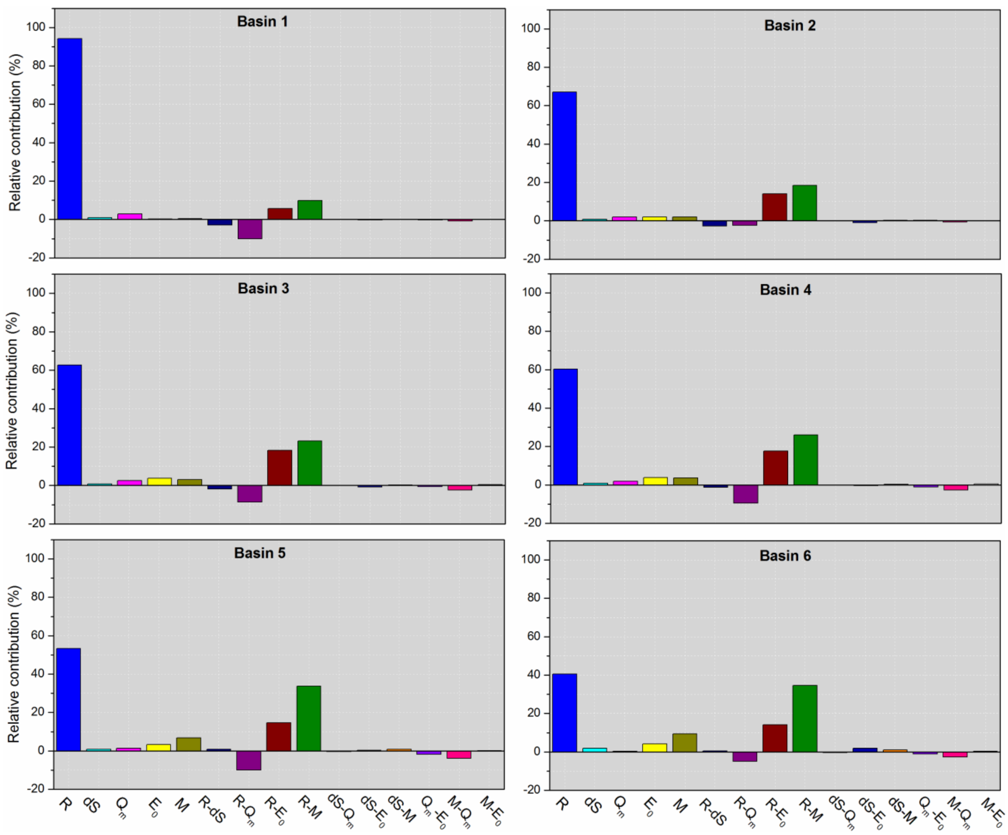

Figure 5 Contribution to the ET variance in the growing season from each component in Equation 15.

5 Conclusion

Recently, several studies have applied a variance decomposition framework based on the Budyko equation to elucidate the dominant driving factors of the ET variance at annual and intra-annual scales by decomposing the intra-annual ET variance into the variance/covariance of P, E_0, and ΔS. Vegetation changes can greatly affect the ET variability, but their effects on the ET variance on finer time-scales was not quantified by this decomposed method. Further, in snow-dependent regions, snowpack stores precipitation in winter and releases water in spring; thus, Q_m plays an important role in the hydrological cycle. Therefore, it is also necessary to consider the role of the Q_m changes on the ET variability.

In this study, six arid alpine basins in the Qilian Mountains of northwest China were chosen as examples. The monthly Q_m during 2001–2014 was estimated using the degree-day model, and the growing season ET was calculated using the water balance equation ($ET = R + Q_s - Q_r - \Delta S$). The controlling parameter n of the Choudhury–Yang equation was found to be closely corrected with M, as estimated by $NDVI$ data. Thus, by combining the Choudhury–Yang equation with the semi-empirical formula between n and M, the growing season σ_{ET}^2 is decomposed into the temporal variance and covariance of R, E_0, ΔS, Q_m, and M. The main results showed that considering Q_m and ΔS in the water balance equation can improve the performance of the Budyko framework in snow-dependent basins on a monthly scale; σ_{ET}^2 was primarily enhanced by the R variance, followed by the coupled R and M and then the coupled R and E_0. The enhancing effects of the variance in M and Q_m cannot be ignored; however, the interactions between R and Q_m, M and Q_m, R and ΔS, and Q_m and E_0 dampened σ_{ET}^2.

https://doi.org/10.5194/hess-2020-535
Preprint. Discussion started: 16 November 2020

Hydrology and Earth System Sciences
Open Access
Discussions

As a simple and effective method, our extended *ET* variance decomposition method has the potential to be widely used to assess the hydrological responses to changes in the climate and vegetation in snow-dependent regions at finer time-scales.

Table 2 The elasticity coefficients of ET for five variables and the standard deviation of each variable for the six basins.

	Elasticity coefficients					Standard deviation						
Basin	ε_R	ε_{Qm}	$\varepsilon_{\Delta S}$	ε_{E_0}	ε_M	σ_R, mm	σ_{Qm}, mm	$\sigma_{\Delta S}$, mm	σ_{E_0}, mm	σ_M	Predicted σ_{ET}, mm	Assessed σ_{ET}, mm
1	0.85	0.85	−0.85	0.06	41.94	34.4	6.0	3.4	25.5	0.05	30.2	31.2
2	0.56	0.56	−0.56	0.16	55.84	40.6	7.0	4.3	24.7	0.07	27.8	30.3
3	0.46	0.46	−0.46	0.20	20.81	42.5	8.5	4.9	23.6	0.21	24.9	27.9
4	0.44	0.44	−0.44	0.19	20.58	40.1	7.2	4.8	23.1	0.21	22.5	25.8
5	0.43	0.43	−0.43	0.19	24.60	39.8	6.3	5.1	22.0	0.25	23.3	25.0
6	0.33	0.33	−0.33	0.18	31.51	41.2	4.0	9.0	23.6	0.21	21.3	24.3

https://doi.org/10.5194/hess-2020-535
Preprint. Discussion started: 16 November 2020

Data availability

Meteorological data are available at http://data.cma.cn/data/detail/dataCode/SURF_CLI_CHN_MUL_DAY_CES_V3.0.html. The runoff records were obtained from the Bureau of Hydrology and Water Resources, Gansu Province. The GLDAS data are available at https://disc.gsfc.nasa.gov/datasets/GLDAS_NOAH025_M_2.0/summary. MODIS MOD10A2 Version 6 snow cover products are available at https://nsidc.org/data/mod10a2. MODIS MOD13A3.006 products are available at https://lpdaac.usgs.gov/products/mod13a3v006/. The land-use map with 1-km resolution in 2010 is available at http://www.resdc.cn/data.aspx?DATAID=99. The Digital elevation data is available at http://www.gscloud.cn/sources/accessdata/310?pid=302.

Author contributions

Tingting Ning: Methodology, Writing–original draft, Software, Visualisation

Zhi Li: Writing–review & editing

Qi Feng: Conceptualisation, Supervision

Zongxing Li and Yanyan Qin: Data curation, Resources

Competing interests

The authors declare that they have no conflicts of interest.

Acknowledgements

This study was supported by the National Natural Science Foundation of China (41807160, U1703124, 42001035), the CAS 'Light of West China' Program (Y929651001), the National Key Research and Development Program of China (2017YFC0404305), and the Major Program of the Natural Science Foundation of Gansu Province, China (18JR4RA002).

References

Barnett, T.P., Adam, J.C.,&Lettenmaier, D.P., 2005. Potential impacts of a warming climate on water availability in snow-dominated regions. *Nature*, 438(7066): 303-309.

Barnhart, T.B., Molotch, N.P., Livneh, B., Harpold, A.A., Knowles, J.F.,&Schneider, D., 2016. Snowmelt rate dictates streamflow. *Geophysical Research Letters*, 43(15): 8006-8016.

Berghuijs, W.R., Larsen, J.R., Van Emmerik, T.H.M.,&Woods, R.A., 2017. A Global

https://doi.org/10.5194/hess-2020-535
Preprint. Discussion started: 16 November 2020

Hydrology and Earth System Sciences Discussions

Assessment of Runoff Sensitivity to Changes in Precipitation, Potential Evaporation, and Other Factors. *Water Resources Research*, 53: 8475-8486.

Bosson, E., Sabel, U., Gustafsson, L.-G., Sassner, M.,&Destouni, G., 2012. Influences of shifts in climate, landscape, and permafrost on terrestrial hydrology. *Journal of Geophysical Research-Atmospheres*, 117: D05120.

Bourque, C.P.A.,&Mir, M.A., 2012. Seasonal snow cover in the Qilian Mountains of Northwest China: Its dependence on oasis seasonal evolution and lowland production of water vapour. *Journal of Hydrology*, 454: 141-151.

Bruemmer, C., Black, T.A., Jassal, R.S., Grant, N.J., Spittlehouse, D.L., Chen, B., Nesic, Z., Amiro, B.D., Arain, M.A., Barr, A.G., Bourque, C.P.A., Coursolle, C., Dunn, A.L., Flanagan, L.B., Humphreys, E.R., Lafleur, P.M., Margolis, H.A., McCaughey, J.H.,&Wofsy, S.C., 2012. How climate and vegetation type influence evapotranspiration and water use efficiency in Canadian forest, peatland and grassland ecosystems. *Agricultural and Forest Meteorology*, 153: 14-30.

Budyko, M.I., 1961. Determination of evaporation from the land surface (in Russian). *Izvestiya Akad.nauk Sssr.ser.geograf.geofiz*, 6: 3-17.

Budyko, M.I., 1974. Climate and life. Academic, New York.

https://doi.org/10.5194/hess-2020-535
Preprint. Discussion started: 16 November 2020

Chen, X., Alimohammadi, N.,&Wang, D., 2013. Modeling interannual variability of seasonal evaporation and storage change based on the extended Budyko framework. *Water Resources Research*, 49(9): 6067-6078.

Choudhury, B.J., 1999. Evaluation of an empirical equation for annual evaporation using field observations and results from a biophysical model. *Journal of Hydrology*, 216(1-2): 99-110.

Cong, Z., Shahid, M., Zhang, D., Lei, H.,&Yang, D., 2017. Attribution of runoff change in the alpine basin: a case study of the Heihe Upstream Basin, China. *Hydrological Sciences Journal-Journal Des Sciences Hydrologiques*, 62(6): 1013-1028.

Deng, S., Yang, T., Zeng, B., Zhu, X.,&Xu, H., 2013. Vegetation cover variation in the Qilian Mountains and its response to climate change in 2000-2011. *Journal of Mountain Science*, 10(6): 1050-1062.

Du, C., Sun, F., Yu, J., Liu, X.,&Chen, Y., 2016. New interpretation of the role of water balance in an extended Budyko hypothesis in arid regions. *Hydrology and Earth System Sciences*, 20(1): 393-409.

Du, J., He, Z., Piatek, K.B., Chen, L., Lin, P.,&Zhu, X., 2019. Interacting effects of temperature and precipitation on climatic sensitivity of spring vegetation green-up in arid mountains of China. *Agricultural and Forest Meteorology*, 269: 71-

https://doi.org/10.5194/hess-2020-535
Preprint. Discussion started: 16 November 2020

77.

Falge, E., Baldocchi, D., Tenhunen, J., Aubinet, M., Bakwin, P., Berbigier, P., Bernhofer, C., Burba, G., Clement, R., Davis, K.J., Elbers, J.A., Goldstein, A.H., Grelle, A., Granier, A., Guomundsson, J., Hollinger, D., Kowalski, A.S., Katul, G., Law, B.E., Malhi, Y., Meyers, T., Monson, R.K., Munger, J.W., Oechel, W., Paw, K.T., Pilegaard, K., Rannik, U., Rebmann, C., Suyker, A., Valentini, R., Wilson, K.,&Wofsy, S., 2002. Seasonality of ecosystem respiration and gross primary production as derived from FLUXNET measurements. *Agricultural and Forest Meteorology*, 113(1-4): 53-74.

Feng, S., Liu, J., Zhang, Q., Zhang, Y., Singh, V.P., Gu, X.,&Sun, P., 2020. A global quantitation of factors affecting evapotranspiration variability. *Journal of Hydrology*, 584: 124688 .

Feng, X., Fu, B., Piao, S., Wang, S.,&Ciais, P., 2016. Revegetation in China's Loess Plateau is approaching sustainable water resource limits. *Nature Climate Change*, 6: 1019-1022.

Gao, X., Zhang, S., Ye, B.,&Gao, H., 2011. Recent changes of glacier runoff in the Hexi Inland river basin. *Advances in Water Science (In Chinese)*, 22(3): 344-350.

Godsey, S.E., Kirchner, J.W.,&Tague, C.L., 2014. Effects of changes in winter snowpacks on summer low flows: case studies in the Sierra Nevada, California,

https://doi.org/10.5194/hess-2020-535
Preprint. Discussion started: 16 November 2020

Hydrology and Earth System Sciences Discussions

USA. *Hydrological Processes*, 28(19): 5048-5064.

Griessinger, N., Seibert, J., Magnusson, J.,&Jonas, T., 2016. Assessing the benefit of snow data assimilation for runoff modeling in Alpine catchments. *Hydrology and Earth System Sciences*, 20(9): 3895-3905.

Hock, R., 2003. Temperature index melt modelling in mountain areas. *Journal of Hydrology*, 282(1-4): 104-115.

Huning, L.S.,&AghaKouchak, A., 2018. Mountain snowpack response to different levels of warming. *Proceedings of the National Academy of Sciences of the United States of America*, 115(43): 10932-10937.

Katul, G.G., Oren, R., Manzoni, S., Higgins, C.,&Parlange, M.B., 2012. Evapotranspiration: a process driving mass transport and energy exchange in the soil-plant-atmosphere-cliamte system. *Reviews of Geophysics*, 50: RG3002.

Koster, R.D.,&Suarez, M.J., 1999. A simple framework for examining the interannual variability of land surface moisture fluxes. *Journal of Climate*, 12(7): 1911-1917.

Lan, Y., Hu, X., Din, H., La, C.,&Song, J., 2012. Variation of Water Cycle Factors in the Western Qilian Mountain Area under Climate WarmingTaking the Mountain Watershed of the Main Stream of Shule River Basin for Example. *Journal of*

https://doi.org/10.5194/hess-2020-535
Preprint. Discussion started: 16 November 2020

Mountain Science （*in Chinese*）, 30(6): 675-680.

Li, B., Chen, Y., Chen, Z.,&Li, W., 2012. The Effect of Climate Change during Snowmelt Period on Streamflow in the Mountainous Areas of Northwest China. *Acta Geographica Sinica* （*In Chinese*）, 67(11): 1461-1470.

Li, D., Pan, M., Cong, Z., Zhang, L.,&Wood, E., 2013. Vegetation control on water and energy balance within the Budyko framework. *Water Resources Research*, 49(2): 969-976.

Li, L.L., Li, J., Chen, H.M.,&Yu, R.C., 2019a. Diurnal Variations of Summer Precipitation over the Qilian Mountains in Northwest China. *Journal of Meteorological Research*, 33(1): 18-30.

Li, S., Zhang, L., Kang, S., Tong, L., Du, T., Hao, X.,&Zhao, P., 2015. Comparison of several surface resistance models for estimating crop evapotranspiration over the entire growing season in arid regions. *Agricultural and Forest Meteorology*, 208: 1-15.

Li, X., Cheng, G., Ge, Y., Li, H., Han, F., Hu, X., Tian, W., Tian, Y., Pan, X., Nian, Y., Zhang, Y., Ran, Y., Zheng, Y., Gao, B., Yang, D., Zheng, C., Wang, X., Liu, S.,&Cai, X., 2018. Hydrological Cycle in the Heihe River Basin and Its Implication for Water Resource Management in Endorheic Basins. *Journal of Geophysical Research-Atmospheres*, 123(2): 890-914.

https://doi.org/10.5194/hess-2020-535
Preprint. Discussion started: 16 November 2020

Li, Z., Feng, Q., Li, Z., Yuan, R., Gui, J.,&Lv, Y., 2019b. Climate background, fact and hydrological effect of multiphase water transformation in cold regions of the Western China: A review. *Earth-Science Reviews*, 190: 33-57.

Li, Z., Feng, Q., Wang, Q.J., Yong, S., Cheng, A.,&Li, J., 2016. Contribution from frozen soil meltwater to runoff in an in-land river basin under water scarcity by isotopic tracing in northwestern China. *Global and Planetary Change*, 136: 41-51.

Liu, J., Zhang, Q., Feng, S., Gu, X., Singh, V.P.,&Sun, P., 2019. Global Attribution of Runoff Variance Across Multiple Timescales. *Journal of Geophysical Research-Atmospheres*, 124(24): 13962-13974.

Liu, J., Zhang, Q., Singh, V.P., Song, C., Zhang, Y.,&Sun, P., 2018. Hydrological effects of climate variability and vegetation dynamics on annual fluvial water balance at global large river basins. *Hydrology & Earth System Sciences*, 22: 4047-4060.

Ma, Z., Kang, S., Zhang, L., Tong, L.,&Su, X., 2008. Analysis of impacts of climate variability and human activity on streamflow for a river basin in arid region of northwest China. *Journal of Hydrology*, 352(3-4): 239-249.

Matin, M.A.,&Bourque, C.P.A., 2015. Mountain-river runoff components and their role in the seasonal development of desert-oases in northwest China. *Journal of Arid Environments*, 122: 1-15.

https://doi.org/10.5194/hess-2020-535
Preprint. Discussion started: 16 November 2020

Maurya, A.S., Rai, S.P., Joshi, N., Dutt, K.S.,&Rai, N., 2018. Snowmelt runoff and groundwater discharge in Himalayan rivers: a case study of the Satluj River, NW India. *Environmental Earth Sciences*, 77(19): 694.

Ning, T., Li, Z., Feng, Q., Chen, W.,&Li, Z., 2020. Effects of forest cover change on catchment evapotranspiration variation in China. *Hydrological Processes*, 34(10): 2219-2228.

Potter, N.J., Zhang, L., Milly, P.C.D., McMahon, T.A.,&Jakeman, A.J., 2005. Effects of rainfall seasonality and soil moisture capacity on mean annual water balance for Australian catchments. *Water Resources Research*, 41(6): W06007.

Priestley, C.,&Taylor, R., 1972. On the assessment of surface heat flux and evaporation using large-scale parameters. *Monthly Weather Review*, 100(2): 81-92.

Qin, Y., Abatzoglou, J.T., Siebert, S., Huning, L.S., AghaKouchak, A., Mankin, J.S., Hong, C., Tong, D., Davis, S.J.,&Mueller, N.D., 2020. Agricultural risks from changing snowmelt. *Nature Climate Change*, 10(5): 459-465.

Ragettli, S., Pellicciotti, F., Immerzeel, W.W., Miles, E.S., Petersen, L., Heynen, M., Shea, J.M., Stumm, D., Joshi, S.,&Shrestha, A., 2015. Unraveling the hydrology of a Himalayan catchment through integration of high resolution in situ data and remote sensing with an advanced simulation model. *Advances in Water Resources*, 78: 94-111.

Rice, R., Bales, R.C., Painter, T.H.,&Dozier, J., 2011. Snow water equivalent along elevation gradients in the Merced and Tuolumne River basins of the Sierra Nevada. *Water Resources Research*, 47: W08515.

Rodriguez-Iturbe, I., 2000. Ecohydrology: A hydrologic perspective of climate-soil-vegetation dynamics. *Water Resources Research*, 36(1): 3-9.

Semadeni-Davies, A., 1997. Monthly snowmelt modelling for large-scale climate change studies using the degree day approach. *Ecological Modelling*, 101(2-3): 303-323.

Stewart, I.T., 2009. Changes in snowpack and snowmelt runoff for key mountain regions. *Hydrological Processes*, 23(1): 78-94.

Stewart, I.T., Cayan, D.R.,&Dettinger, M.D., 2005. Changes toward earlier streamflow timing across western North America. *Journal of Climate*, 18(8): 1136-1155.

Villegas, J.C., Breshears, D.D., Zou, C.B.,&Law, D.J., 2010. Ecohydrological controls of soil evaporation in deciduous drylands: How the hierarchical effects of litter, patch and vegetation mosaic cover interact with phenology and season. *Journal of Arid Environments*, 74(5): 595-602.

Wagle, P.,&Kakani, V.G., 2014. Growing season variability in evapotranspiration, ecosystem water use efficiency, and energy partitioning in switchgrass.

https://doi.org/10.5194/hess-2020-535
Preprint. Discussion started: 16 November 2020

Ecohydrology, 7(1): 64-72.

Wang, D.,&Hejazi, M., 2011. Quantifying the relative contribution of the climate and direct human impacts on mean annual streamflow in the contiguous United States. *Water Resources Research*, 47: W00J12.

Wang, J., Li, H.,&Hao, X., 2010a. Responses of snowmelt runoff to climatic change in an inland river basin, Northwestern China, over the past 50 years. *Hydrology and Earth System Sciences*, 14(10): 1979-1987.

Wang, J.,&Li, S., 2005. The influence of climate change on snowmelt runoff variation in arid alpine regions of China. *Science in China (In Chinese)*, 35(7): 664-670.

Wang, J.,&Li, W., 2001. Establishing snowmelt runoff simulating model using remote sensing data and GIS in the west of China. *International Journal of Remote Sensing*, 22(17): 3267-3274.

Wang, K., Wang, P., Li, Z., Cribb, M.,&Sparrow, M., 2007. A simple method to estimate actual evapotranspiration from a combination of net radiation, vegetation index, and temperature. *Journal of Geophysical Research-Atmospheres*, 112(D15): D15107.

Wang, L., Caylor, K.K., Villegas, J.C., Barron-Gafford, G.A., Breshears, D.D.,&Huxman, T.E., 2010b. Partitioning evapotranspiration across gradients

https://doi.org/10.5194/hess-2020-535
Preprint. Discussion started: 16 November 2020

of woody plant cover: Assessment of a stable isotope technique. *Geophysical Research Letters*, 37: L09401.

Wang, R., Yao, Z., Liu, Z., Wu, S., Jiang, L.,&Wang, L., 2015. Snow cover variability and snowmelt in a high-altitude ungauged catchment. *Hydrological Processes*, 29(17): 3665-3676.

Wang, Y.-J.,&Qin, D.-H., 2017. Influence of climate change and human activity on water resources in arid region of Northwest China: An overview. *Advances in Climate Change Research*, 8(4): 268-278.

Wei, X., Li, Q., Zhang, M., Giles-Hansen, K., Liu, W., Fan, H., Wang, Y., Zhou, G., Piao, S.,&Liu, S., 2018. Vegetation cover-another dominant factor in determining global water resources in forested regions. *Global Change Biology*, 24(2): 786-795.

Wu, C., Hu, B.X., Huang, G.,&Zhang, H., 2017. Effects of climate and terrestrial storage on temporal variability of actual evapotranspiration. *Journal of Hydrology*, 549: 388-403.

Wu, F., Zhan, J., Wang, Z.,&Zhang, Q., 2015. Streamflow variation due to glacier melting and climate change in upstream Heihe River Basin, Northwest China. *Physics and Chemistry of the Earth*, 79-82: 11-19.

https://doi.org/10.5194/hess-2020-535
Preprint. Discussion started: 16 November 2020

Hydrology and Earth System Sciences
Discussions

Xu, C.Y.,&Singh, V.P., 2005. Evaluation of three complementary relationship evapotranspiration models by water balance approach to estimate actual regional evapotranspiration in different climatic regions. *Journal of Hydrology*, 308(1-4): 105-121.

Xu, X., Liu, W., Scanlon, B.R., Zhang, L.,&Pan, M., 2013. Local and global factors controlling water-energy balances within the Budyko framework. *Geophysical Research Letters*, 40(23): 6123-6129.

Yang, D., Shao, W., Yeh, P.J.F., Yang, H., Kanae, S.,&Oki, T., 2009. Impact of vegetation coverage on regional water balance in the nonhumid regions of China. *Water Resources Research*, 45: W00A14.

Yang, D.W., Sun, F.B., Liu, Z.T., Cong, Z.T.,&Lei, Z.D., 2006. Interpreting the complementary relationship in non-humid environments based on the Budyko and Penman hypotheses. *Geophysical Research Letters*, 33(18): L18402.

Yang, H.B., Yang, D.W., Lei, Z.D.,&Sun, F.B., 2008. New analytical derivation of the mean annual water-energy balance equation. *Water Resources Research*, 44(3): W03410.

Yang, L., Feng, Q., Yin, Z., Wen, X., Si, J., Li, C.,&Deo, R.C., 2017. Identifying separate impacts of climate and land use/cover change on hydrological processes in upper stream of Heihe River, Northwest China. *Hydrological*

https://doi.org/10.5194/hess-2020-535
Preprint. Discussion started: 16 November 2020

Processes, 31(5): 1100-1112.

Yang, T., Wang, C., Chen, Y., Chen, X.,&Yu, Z., 2015. Climate change and water storage variability over an arid endorheic region. *Journal of Hydrology*, 529: 330-339.

Ye, S., Li, H.-Y., Li, S., Leung, L.R., Demissie, Y., Ran, Q.,&Bloeschl, G., 2015. Vegetation regulation on streamflow intra-annual variability through adaption to climate variations. *Geophysical Research Letters*, 42(23): 10307-10315.

Ye, S., Li, H.Y., Li, S., Leung, L.R., Demissie, Y., Ran, Q.,&Blöschl, G., 2016. Vegetation regulation on streamflow intra-annual variability through adaption to climate variations. *Geophysical Research Letters*, 42(23): 10,307-10,315.

Yuan, W., Liu, S., Liu, H., Randerson, J.T., Yu, G.,&Tieszen, L.L., 2010. Impacts of precipitation seasonality and ecosystem types on evapotranspiration in the Yukon River Basin, Alaska. *Water Resources Research*, 46: W02514.

Zeng, R.,&Cai, X., 2015. Assessing the temporal variance of evapotranspiration considering climate and catchment storage factors. *Advances in Water Resources*, 79: 51-60.

Zeng, R.,&Cai, X., 2016. Climatic and terrestrial storage control on evapotranspiration temporal variability: Analysis of river basins around the world. *Geophysical*

Research Letters, 43(1): 185-195.

Zhang, D., Cong, Z., Ni, G., Yang, D.,&Hu, S., 2015. Effects of snow ratio on annual runoff within the Budyko framework. *Hydrology and Earth System Sciences*, 19(4): 1977-1992.

Zhang, D., Liu, X., Zhang, Q., Liang, K.,&Liu, C., 2016a. Investigation of factors affecting intra-annual variability of evapotranspiration and streamflow under different climate conditions. *Journal of Hydrology*, 543: 759-769.

Zhang, S., Yang, H., Yang, D.,&Jayawardena, A.W., 2016b. Quantifying the effect of vegetation change on the regional water balance within the Budyko framework. *Geophysical Research Letters*, 43(3): 1140-1148.

Zhang, Y., Luo, Y., Sun, L., Liu, S., Chen, X.,&Wang, X., 2016c. Using glacier area ratio to quantify effects of melt water on runoff. *Journal of Hydrology*, 538: 269-277.

Zhou, S., Yu, B., Huang, Y.,&Wang, G., 2015. The complementary relationship and generation of the Budyko functions. *Geophysical Research Letters*, 42(6): 1781-1790.